Opto-Electronic Advances

CN 51−1781/TN ISSN 2096−4579 (Print) ISSN 2097−3993 (Online)

Separation and identification of mixed signal for distributed acoustic sensor using deep learning

Huaxin Gu, Jingming Zhang, Xingwei Chen, Feihong Yu, Deyu Xu, Shuaiqi Liu, Weihao Lin, Xiaobing Shi, Zixing Huang, Xiongji Yang, Qingchang Hu and Liyang Shao

Citation: Gu HX, Zhang JM, Chen XW, et al. Separation and identification of mixed signal for distributed acoustic sensor using deep learning. *Opto-Electron Adv* **8**, 240270(2025).

https://doi.org/10.29026/oea.2025.240270

Received: 14 November 2025; Accepted: 3 September 2025; Published online: 10 November 2025

Related articles

Physics-informed deep learning for fringe pattern analysis
Wei Yin, Yuxuan Che, Xinsheng Li, Mingyu Li, Yan Hu, Shijie Feng, Edmund Y. Lam, Qian Chen, Chao Zuo
Opto-Electronic Advances 2024 **7**, 230034 doi: 10.29026/oea.2024.230034

Adaptive decentralized AI scheme for signal recognition of distributed sensor systems
Shixiong Zhang, Hao Li, Cunzheng Fan, Zhichao Zeng, Chao Xiong, Jie Wu, Zhijun Yan, Deming Liu, Qizhen Sun
Opto-Electronic Advances 2024 **7**, 240119 doi: 10.29026/oea.2024.240119

More related article in Opto-Electronic Journals Group website

Opto-Electronic Advances

Article
November 2025, Vol. 8, No. 11

DOI: 10.29026/oea.2025.240270 CSTR: 32247.14.oea.2025.240270

Separation and identification of mixed signal for distributed acoustic sensor using deep learning

Huaxin Gu[1], Jingming Zhang[2], Xingwei Chen[2], Feihong Yu[2], Deyu Xu[1], Shuaiqi Liu[3], Weihao Lin[4], Xiaobing Shi[2], Zixing Huang[2], Xiongji Yang[2], Qingchang Hu[2] and Liyang Shao[1,2,5]*

With the application of Distributed Acoustic Sensors (DAS) across various infrastructures, it will play a pivotal role in shaping smart cities in the future. However, the current single-source detection and identification technology might struggle to meet the high precision needs in the intricate environmental conditions of mixed multi-source interference. We propose a new deep neural network-based multi-source signal separation method for DAS and accomplish the separation performance of this method under practical applications. In addition, a new evaluation metric for the separation method is proposed in conjunction with the separation and identification of DAS mixed signals. For mixed signals with different source numbers, the recognizable rate of separated signals can reach 98.33% on average. This study provides a promising solution to the multi-source mixed interference problem faced by DAS in complex environments.

Keywords: distributed acoustic sensor; deep learning; multi-source separation; pattern recognition

Gu HX, Zhang JM, Chen XW et al. Separation and identification of mixed signal for distributed acoustic sensor using deep learning. *Opto-Electron Adv* **8**, 240270 (2025).

Introduction

Distributed fiber optic sensors based on phase-sensitive optical time-domain reflectometry (Φ-OTDR) represent an advanced sensing technology that makes use of fiber optics for the detection of vibrations in areas along the lines of transmission. These sensors offer a variety of advantages, including long-distance sensing, resistance to electromagnetic interference, high-sensitivity distributed detection[1–5], etc. Over the past decade, significant research has been conducted to enhance the sensitivity[6], detection range[7,8], frequency response range[9], intrusion event detection accuracy[10], and massive data set storage techniques[11] for DAS systems. These advancements have facilitated the application of DAS technology in practical fields, including perimeter security[12,13], the detection of long-distance pipelines[14], mining transporters[15], and sandstone aquifers[16]. It is noteworthy that the advancement of communication and sensing technologies on a single optical fiber simultaneously paves the way for the integration of the DAS system into a vast communication cable network, alongside the construction of a comprehensive optical fiber sensing network on a grand

[1]School of Innovation and Entrepreneurship, Southern University of Science and Technology, Shenzhen 518055, China; [2]Department of Electrical and Electronic Engineering, Southern University of Science and Technology, Shenzhen 518055 China; [3]Zhengzhou Research Institute, Harbin Institute of Technology, Zhengzhou 450000, China; [4]Higher Educational Key Laboratory for Flexible Manufacturing Equipment Integration of Fujian Province; School of Mechanical Electrical and Information Engineering, Xiamen Institute of Technology, Xiamen 361021, China; [5]Peng Cheng Laboratory, Shenzhen 518055, China.

*Correspondence: Shao LY, E-mail: shaoly@sustech.edu.cn

Received: 14 November 2025; Accepted: 3 September 2025; Published online: 10 November 2025

scale. It seems reasonable to state that DAS technology is going to become an important pillar in the construction of the digital world of the future. However, during the detection process, DAS systems inevitably have to cope with complex environments and simultaneous interference from multiple intrusion events which pose some challenges to the precise detection and recognition of target vibration signals.

In previous studies, researchers have done a lot of work based on machine learning models and deep learning models for the single source signal identification of DAS systems[17]. The main machine learning-based DAS signal recognition models are the Support Vector Machine (SVM)[18,19] and the Hidden Markov Model (HMM)[20,21]. Fouda et al. combined time-frequency domain features with SVM classifiers to identify malicious attacks suffered by multiple submarine cables, and the classification accuracy of three typical events reached more than 96%[18]. A HMM-based dynamic time sequence recognition and knowledge exploitation method is proposed. The measured data show that the average recognition accuracy is as high as 98.2% for five typical events common along buried pipelines[21]. On the other hand, deep learning models can automatically learn features from raw data and perform efficient pattern recognition, so they are also widely adopted by researchers. Lyu et al. proposed a robust intrusion event recognition scheme based on a convolutional prototype network. In the field experiments, the average detection accuracy of the known class of intrusion events can reach 84.67%, and the rejection rate of the unknown class of intrusion events is about 83.75%[22]. Xu et al. proposed a real-time multi-class interference detection algorithm based on YOLO using the Darknet53 network for simultaneous event localization and classification, which can locate and classify intrusion events in real time while achieving an accuracy rate of 96.14%[23]. For the DAS open event classification model, a robust intrusion event detection scheme based on a 1D convolutional neural network with residual learning and the OpenMax algorithm is proposed. The experimental results show that the classification accuracy of this recognition model is greatly improved compared with the traditional 1D CNN signal classification method[24]. Despite the advancement of single-source identification technology for DAS signals, these methods may not be sufficiently robust for high-precision detection in practical applications involving the interference of multiple signals.

At present, the main solution idea for the problem of multi-source mixed interference in DAS systems is to separate the mixed signals. According to the number of sensor channels used in the separation, it can be divided into two kinds of mixed-signal separation methods, multi-sensor channel and single-sensor channel. In 2022, Wu et al. proposed a source number judgment method for the mixed signals under unknown source numbers and unknown mixing conditions. They used the improved FastICA method to successfully achieve the separation of multi-source signals under the linear aliasing model and employed a variety of metrics to evaluate the separated results. This is also the first work that achieved the separation of different source signals on DAS-aliased signals[25]. Furthermore, they put forth the xSFA method for the separation of mixed signals and validated the efficacy in both laboratory and outdoor settings. This study was based on the observation that the multi-source signals in real-world environments are more compatible with nonlinear aliasing[26]. In 2023, we used the FastIVA method to achieve two-source mixed signal separation within laboratory conditions[27]. All of the above three methods are multi-sensor channel-based signal separation methods, which require more mixed signals than the number of mixed sources. Therefore, there are some limitations in some special scenarios. There is also some progress in the separation research of DAS signals using single-sensor channels. Luo et al.[28] used the DAS system to conduct experiments based on ultra-weak fiber Bragg Grating within laboratory conditions. They constructed the dataset of DAS mixed signals for the first time and achieved the separation of two-source and three-source mixed signals by using the deep learning network Conv-TasNet. The corresponding time-frequency entropy (TFE) similarities of the three-source (knocking, steel pipe friction, and fan vibration) separation results reached 97.5%, 92.8%, and 90.2%, which verified the effectiveness of the method using the deep learning model. However, the work only performed experiments under laboratory conditions and did not verify the stability of the proposed method under external field conditions. Moreover, the above-mentioned works on the separation of DAS mixed signals give the evaluation method of the results but do not directly identify the separation results, which is still blank in the research.

To address the challenges identified, this paper introduces a model for separating multi-source mixed signals in a single-channel DAS framework, utilizing a Dual-Path

Recurrent Neural Network (DPRNN). By investigating the nonlinear mixed model during acoustic signal propagation, we develop training data that reflects real-world conditions more accurately, thereby significantly improving separation performance. The feasibility of our proposed method is confirmed through mixed signals collected from both indoor and outdoor environments.

Recognizing the limitations of existing metrics for evaluating the effectiveness of overlapping signal separation, which hinder accurate assessment, we innovatively integrate the evaluation of post-separation signal quality with signal classification. Specifically, we employ the accuracy of signal clustering as a new metric, enabling a comprehensive assessment of the similarity between the separated signals and the original ones within a higher-dimensional feature space. Under this new metric, our results demonstrate the superiority of the proposed algorithm. In the outdoor experiments, the metric of the two-source mixed signals reached 94.44% and 100%, and the average metric of the three-source mixed signals reached 98.3%. presenting a fresh perspective for addressing multi-source interference issues in practical DAS applications.

Operation principle

Sensing principle of DAS based on Φ-OTDR

DAS systems based on Φ-OTDR are used in a wide range of applications because they provide a continuous, full-time mean of vibration detection in the vicinity of optical fibers. Figure 1 illustrates the typical DAS detection structure. Light from a narrow linewidth laser (NLL) is split at an optical coupler (OC1), resulting in 90% of the light being used for detection and 10% for reference. The acousto-optic modulator (AOM) converts the detection light into probe pulses that are controlled by an arbitrary waveform generator (AWG). Before being injected into the fiber under test (FUT), the probe pulse is amplified by an erbium-doped fiber amplifier (EDFA1) and then passed through a circulator (CIR). The RBS light traveling in the opposite direction is then amplified by another EDFA after the circulator. Noise from the spontaneous emissions of both EDFAs is attenuated by a fiber Bragg grating (FBG). The RBS light then converges with the reference light at OC2, producing a beat signal. This beat signal is detected by a balanced photodetector (BPD). The resulting electrical signals from the BPD are acquired by a data acquisition (DAQ) system and then passed to the personal computer (PC). When vibrations occur around the FUT, the PC receives the signals and demodulates them to restore the vibration signal. The critical parameters of the DAS system employed in the subsequent experiments include a laser pulse width of 100 ns, which corresponds to a spatial resolution of 10 m, along with a sampling rate of 1000 Hz. To mitigate the volume of data collected, the sampling interval has been downsampled to 10 m.

Signal nonlinear aliasing model

In practical scenarios, vibration signals reaching the sensing fiber will inevitably produce various non-linear effects[29], such as absorption attenuation, due to the inhomogeneous propagation medium and reflections from various layers of ground structures and obstacles. Therefore, the signals received by the DAS system are the result of the nonlinear superposition of various types of single-source vibration signals[26]. This multipath superposition process is shown in Fig. 2.

In this case, the signal X_j received at each fiber optic sensing point can be expressed as Eq. (1):

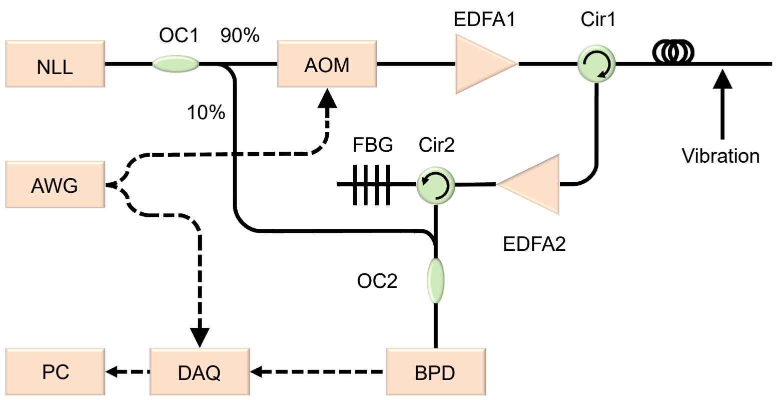

Fig. 1 | The classic DAS system architecture.

$$X_j = \sum_{i=1}^{N} b_{ij}(t) * S_i(t) + v_j(t) = \sum_{i=1}^{N}\sum_{\tau=0}^{L-1} b_{ij}(\tau) * S_i(t-\tau) + v_j(t). \tag{1}$$

here, $*$ represents convolution, $b_{ij}(\tau)$ represents the impulse response used to describe the propagation of the i-th vibration signal to the j-th sensing point, $v_j(t)$ denotes environmental noise, and L is used to describe the filter order of each transmission channel.

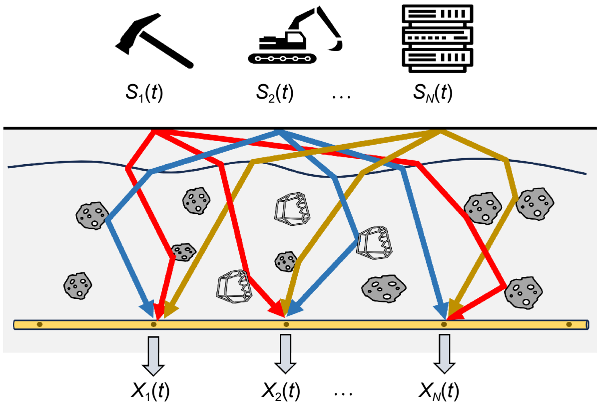

Fig. 2 | Nonlinear aliasing model of DAS signals.

DPRNN model

In this study, the DPRNN, initially proposed by Luo et al[30], is employed for the separation of DAS mixed signals. The DPRNN has demonstrated excellent performance in the separation of mixed audio signals and may prove useful for separation tasks in other domains. It is a deep learning network that processes long time series signals in a multilayer network structure, employing RNN blocks. It adopts an encoder-separator-decoder structure, as shown in Fig. 3. Firstly, the encoder splits and splices the temporal signal into a three-dimensional (3D) tensor; then the 3D tensor is modeled locally and globally using a separator, which is used to estimate the signal mask; finally, a decoder is used to convert the resulting 3D tensor back into a temporal signal. For detailed information on the principles underlying the DPRNN network and its associated loss function, refer to Section 1 of the Supplementary information (SI).

DPRNN experimental scenario

In order to verify the performance of the DPRNN network in separating real mixed signals, we perform three different sets of mixed-signal separation experiments in the laboratory and in the 'Campus Lifeline Project', respectively. The structure of the experiment in laboratory is shown in Fig. 4. The 3 km optical fiber is connected to the DAS system and about 10 m optical fiber is taped to a wooden board of uniform medium at 1 km from the end of the optical fiber with adhesive tape.

In the 'Campus Lifeline Project', the optical fiber is connected from the DAS system placed in the laboratory. It enters the campus optical fiber network in the basement server room, passes through the student dormitory and teaching buildings, and ends at the school conference center, with a total length of 4.8 km. The schematic diagram is shown in Fig. 5.

In these two scenarios, a dataset of DAS aliased signals was constructed. The dataset consists of three independent vibration events: hammer striking vibrations (HS),

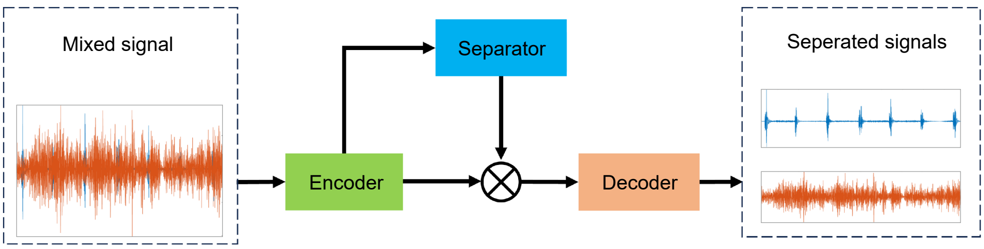

Fig. 3 | DAS mixed signal separation flow.

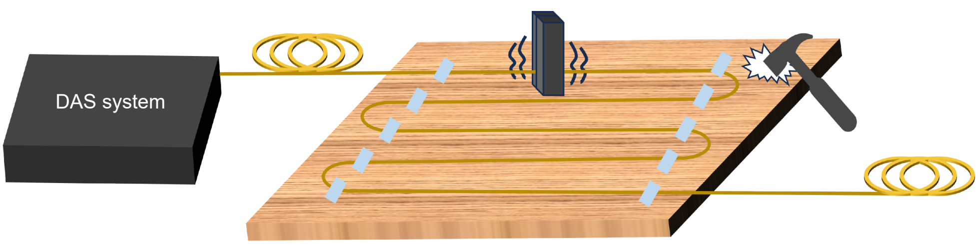

Fig. 4 | Schematic diagram of laboratory experimental setup.

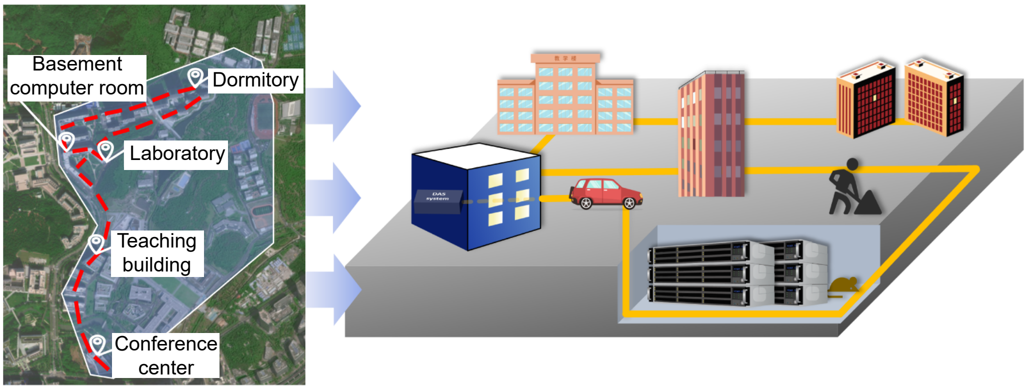

Fig. 5 | Schematic diagram of 'Campus Lifeline Project' based on DAS system.

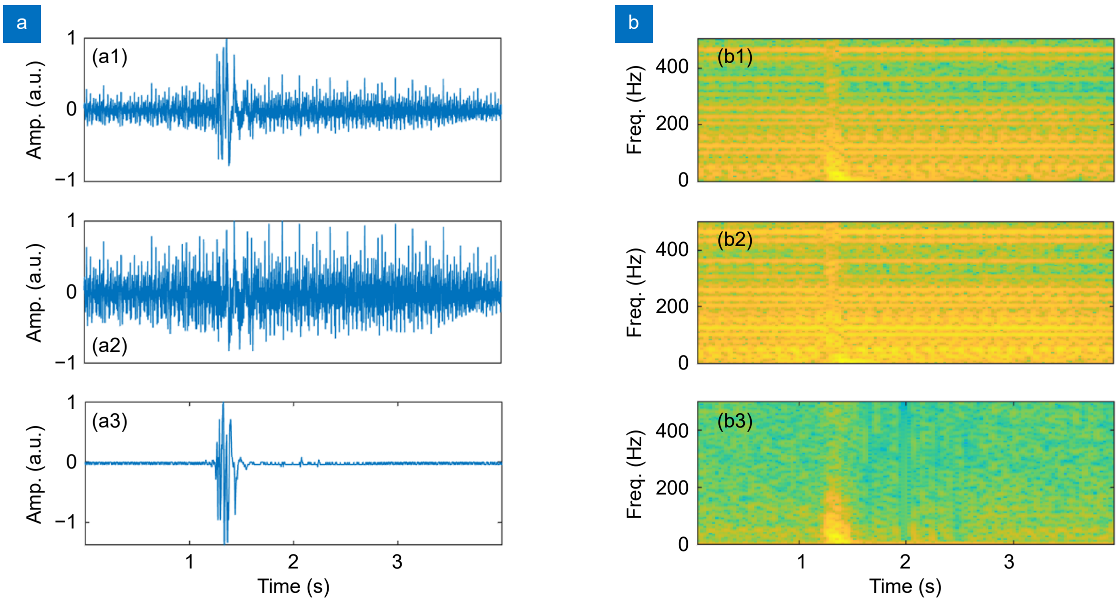

Fig. 6 | Experimental results in separating two-source mixed signals in the laboratory. (**a**) Time-domain signals. (**b**) Time-frequency domain signals. (a1, b1) Two-source mixed signal. (a2, b2) Separated signal (PZTv). (a3, b3) Separated signal (HS).

piezoelectric transducer vibrations (PZTv), and server room background noise (SRBN). These signals were utilized in various combinations for training models. Detailed information regarding the dataset and model training can be found in Sections 2 and 3 of the SI.

Mixed signal separation experiment

Although the training loss above reaches convergence and to some extent shows the separation effect of the DPRNN network for DAS mixed signals, real signals separation experiments are still needed to directly verify the effectiveness of the method. Here we do a total of three different sets of experiments to validate the method's ability to separate real mixed signals. Moreover, we compare all the experimental results obtained by the DPRNN and Conv-TasNet network previously applied to DAS to verify the reliability of our method.

In-lab mixed signal separation experiments with two sources

During the experiment, the PZT is clamped onto the measured optical fiber while a hammer is used to strike the wooden board. A total of 30 mixed signals are collected in the experiment, each of which has a length of 4 s. The mixed data are then processed using the above-trained separation model.

The separation results are evaluated using TFE. It is pointed out in the previous study that the TFE calculation based on Hilbert-Huang transform has problems such as end effect and modal aliasing, so the TFE calculation method based on STFT is more recommended[26].

The flow of this calculation method is as follows:

Step 1: Perform STFT on the signal to obtain the time-frequency spectrum of the signal;

Step 2: The obtained time-frequency spectrum is

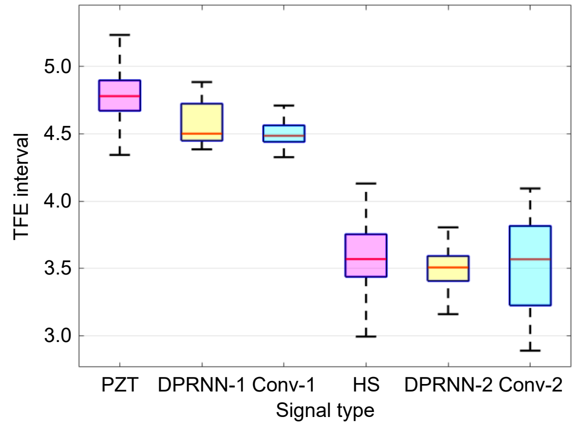

Fig. 7 | Evaluation of the separation effect using TFE in the laboratory ('Conv' for Conv-TasNet).

divided into N time-frequency blocks of equal area, and the energy of each block is w_i, and the energy of the whole plane is A. The normalized energy of each block is obtained by $q_i = w_i/A$;

Step 3: The TFE of this signal is calculated by Eq. (2).

$$s(q) = -\sum_{i=1}^{N} q_i \ln q_i \ . \tag{2}$$

Using the TFE of 2,000 individual signals collected during dataset creation as reference data, the TFE range for PZTv signals is 4.34–5.24, while the range for Striking signals is 2.99–4.13. The two intervals clearly indicate a difference in the ranges of these two data types. If the estimated signals obtained from separation also exhibit significant differences and correspond to each other, it will demonstrate that the algorithm has successfully separated the mixed signals.

Figure 6 presents the separation results of the DPRNN model. The signals in Fig. 6(a2, b2) are very similar to a single PZTv signal in both the time and time-frequency domain, while Fig. 6(a3, b3) resemble the HS signal. To quantitatively verify the effectiveness of the separation, this study inputted 30 sets of mixed signals into the DPRNN model and the Conv-TasNet model, calculating the TFE outputs, as illustrated in Fig. 7. Table 1 presents the specific numerical values corresponding to those shown in Fig. 7. From the perspective of the TFE intervals, the signals separated by each method are similar to a typical single signal. For the estimated signal S_1, the signals separated by DPRNN and Conv-TasNet are almost entirely within the reference range of the typical signal-PZTv. However, the results from DPRNN show a better overlap with the original reference interval, and the Q_1, Q_3, and median of the interval are closer to the values of the reference range. For the estimated signal S_2, the result interval from DPRNN is also entirely within the reference range of the typical signal-striking, with the average difference of Q_1, Q_3, and median from the reference interval being 0.08. The results from Conv-TasNet deviate from the reference interval, with the aforementioned average difference being 0.11.

Under the laboratory conditions of this set of experiments, the nonlinear mixing of signals is weak, as the field conditions are relatively stable and simple. Vibration propagation also occurs through uniform medium wooden boards, resulting in no significant differences between the outcomes of the two methods, although the DPRNN model still demonstrates an advantage.

Experiments on two-source mixed signal separation in the engineering environment

To further verify the ability of the method to be applied in a real environment, we set up a two-source separation experiment in the underground server room. In the underground server room, there are large servers and air conditioning units that continuously interfere with the optical fibers, which can be collectively categorized as

Table 1 | TFE statistics data.

	Category	Interval	Q1*	Q3*	Med*
S1	PZTv	4.34–5.24	4.67	4.90	4.78
	DPRNN	4.39–4.89	4.45	4.72	4.50
	Conv-TasNet	4.33–4.71	4.44	4.56	4.49
S2	HS	2.99–4.13	3.44	3.75	3.57
	DPRNN	3.16–3.81	3.41	3.59	3.51
	Conv-TasNet	2.89–4.10	3.23	3.82	3.57

*Q1 is the first Quartile of the data.

*Q3 is the third Quartile of the data.

*Med is the median of the data.

environmental noise vibrations. When a hammer strikes the ground around the optical fiber, it experiences two types of interference: the impact from the hammer and the surrounding environmental noise, as shown in Fig. 8. Due to the high level of current environmental noise, the striking signal is easily masked and cannot be recognized by the system; therefore, it is necessary to separate the collected mixed vibrations. For the experiments, a total of 144 mixed signals are collected for 4 s each and separated using the trained separation model of HS-SRBN. Figure 9 illustrates the separation results of the DPRNN network for the real two-source mixed signal.

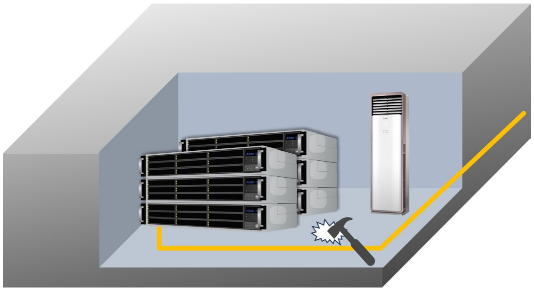

Fig. 8 | Diagram of Two-source mixing experiment in the underground server room.

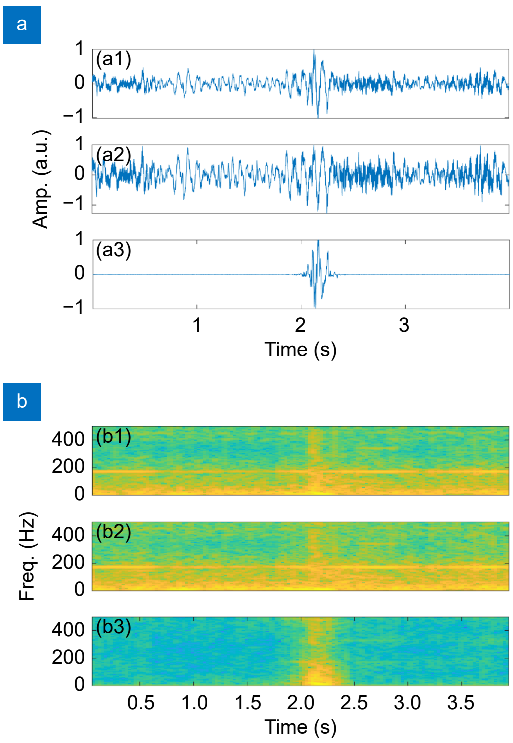

Fig. 9 | Experimental results of two-source mixed signal in the server room. (**a**) Time-domain signals. (**b**) Time-frequency domain signals. (a1, b1) Two-source mixed signal. (a2, b2) Separated signal (SRBN). (a3, b3) Separated signal (HS).

Since the TFE of the two signal types in this experiment overlaps substantially, we assess the model's performance using the SVM-based Recognizable Rate of Separated Signals(RRSS). Regarding the RRSS method, a discussion and details of the computational methods are provided in Section 4 of the Supplementary information (SI).

We use 400 labeled signals to calculate the classification accuracy of the trained SVM model, at which point we obtain a model classification accuracy of 100%. This accuracy is due to the fact that the two signals we classified are relatively different in terms of features. Subsequently, the DPRNN separation results are classified and Fig. 10. shows the scatter plot of the distribution of the two estimated signals based on kurtosis and standard deviation after classifying the signals using SVM. As can be seen, the estimated signals can be classified into two classes, but there are still some misclassifications since only two feature dimensions are drawn here. After the SVM model classification and identification of eight feature dimensions, the RRSSs are obtained as 94.44% and 100% respectively. When the same SVM model processed the results obtained from Conv-TasNet, the RRSSs are 93.75% and 29.86%, respectively, with an average value of 36% over the results of DPRNN. The statistical results are presented in Fig. 11. At this point, we can conclude that the separation method based on DPRNN fulfills the task of separating the two-source signals of DAS in the practical application environment, and the results have obvious advantages compared with the previous methods.

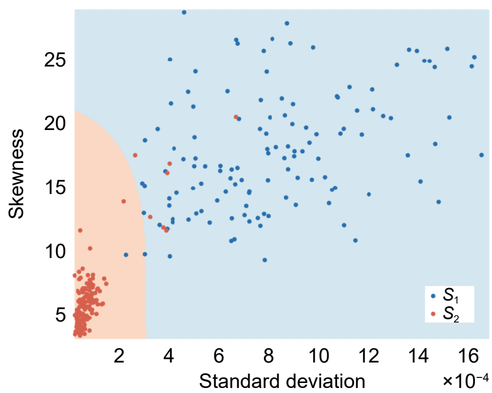

Fig. 10 | Distribution of separation results based on power spectrum standard deviation and skewness.

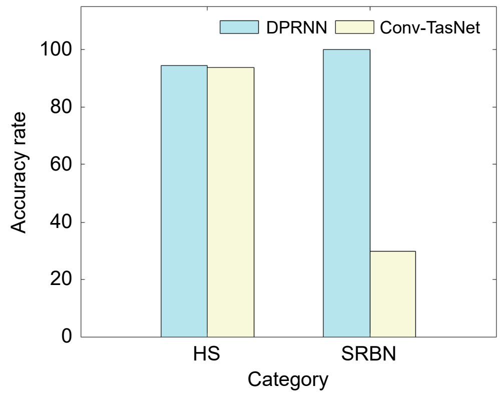

Fig. 11 | Comparison of the two methods in terms of the RRSS (Case B).

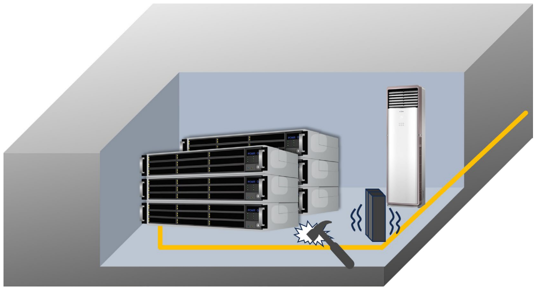

Fig. 12 | Diagram of three-source mixing experiment in the underground server room.

Experiments on three-source mixed signal separation in the engineering environment

The effectiveness of the method for the separation of three-source signals should also be verified directly, therefore, we conduct the three-source signal mixing experiments in the server room environment to test the processing effect of the method under different source numbers. In the server room environment, hammer strikes and PZT interference are simultaneously performed around the sensing fiber, at which time the sensing signal collected by the DAS system is a three-source mixture. The experimental scene is illustrated as shown in the Fig. 12.

120 samples are collected of 4 s each and processed using the trained three-source separation model. Figure 13 illustrates the results of the DPRNN network separation.

From the time and time-frequency domains, the DPRNN network performs a relatively satisfactory separation of the three source signals in the real environment. Each of the three estimation results corresponds to each other with the expected three signals, but the effect of the separation still needs to be quantified. Since there is a high overlap in TFE for two of the signals, we also use the RRSS proposed in the previous section for the evaluation of the model's effectiveness. At this point, according to the calculation process of RRSS, the accuracy of the SVM is calculated to be 98%. The 360 signals obtained from the DPRNN separation are inputted into the SVM. It can be seen from Fig. 14 that the three separated signals have a clear distribution trend, which verifies the effectiveness of the method in two feature dimensions. The RRSSs of the DPRNN network are 100%, 100%, and 95%. The three results for the Conv-TasNet network with the same data and SVM model are 55%, 99.17%, and 98.33%. In terms of the mean value of RRSS, DPRNN is 14 % higher than Conv-TasNet. From the results in Fig. 15, the DPRNN network is better than the Conv-TasNet network for DAS mixed signal separation. The fidelity analysis of separating three-source aliased signals is presented in Section 5 of the SI.

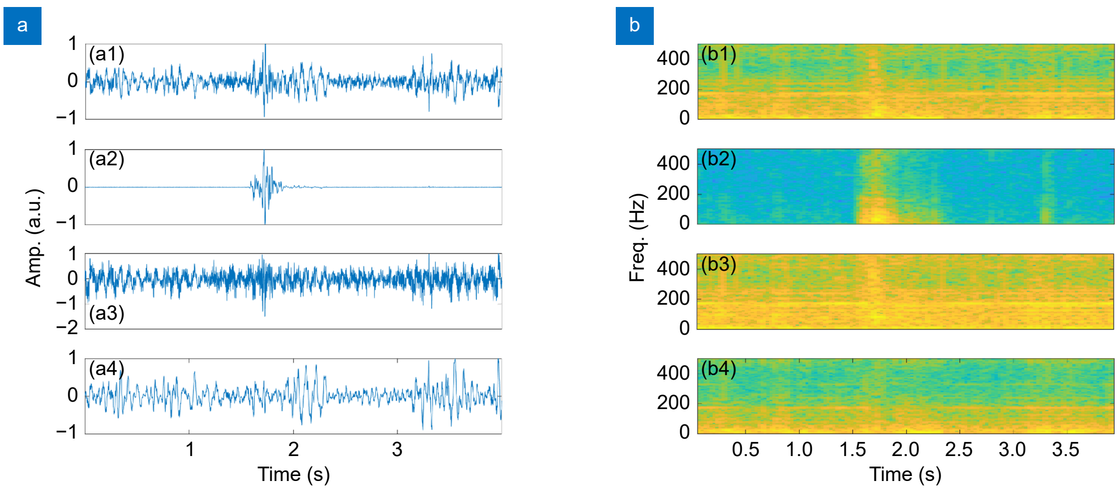

Fig. 13 | Experimental results of three-source mixed signal in the server room. (**a**) Time-domain signals. (**b**) Time-frequency domain signals. (a1, b1) Three-source mixed signal. (a2, b2) Separated signal (HS). (a3, b3) Separated signal (PZTv). (a4, b4) Separated signal (SRBN).

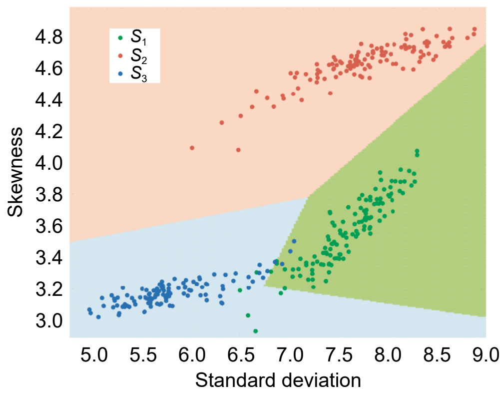

Fig. 14 | Distribution of three-source separation results based on power spectrum standard deviation and skewness.

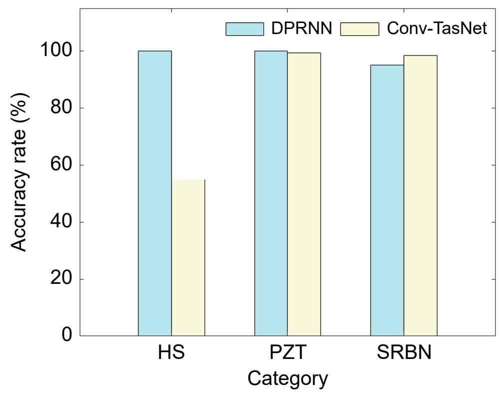

Fig. 15 | Comparison of the two methods in terms of the RRSS.

Up to this point, we have completed three sets of experiments in the laboratory and in a real engineering environment. The separation performance of DPRNN network for two-source and three-source mixed signals of DAS is verified.

Conclusions

This study introduces the application of DPRNN for separating nonlinear mixed interference signals in DAS across diverse environments. Furthermore, we propose the utilization of SVM to directly assess the separation outcomes, thereby circumventing the challenge of evaluating individual signals when they overlap in the TFE. To validate the separation efficacy and stability of the DPRNN network, we have designed three experimental sets, focusing on various scenarios and differing numbers of mixed sources. The experimental results demonstrate that the DPRNN network surpasses the Conv-TasNet network in three distinct experiments, according to two different evaluation metrics. Specifically, in terms of the mean value of RRSS, DPRNN exhibits an improvement of 36% and 14% in two-source and three-source mixing scenarios, achieving accuracies of 97.22% and 98.33%. Consequently, we are justified in concluding that the integration of DPRNN and SVM holds promise for advancing the resolution of multi-source mixed interference issues in DAS across various practical applications. This combined approach has the potential to overcome the current limitations in the application promotion of DAS technology.

References

1. Bao XY, Wang Y. Recent advancements in Rayleigh scattering-based distributed fiber sensors. *Adv Dev Instrum* **2021**, 8696571 (2021).
2. He ZY, Liu QW. Optical fiber distributed acoustic sensors: a review. *J Lightwave Technol* **39**, 3671–3686 (2021).
3. Rao YJ, Wang ZN, Wu HJ et al. Recent advances in phase-sensitive optical time domain reflectometry (Φ-OTDR). *Photonic Sens* **11**, 1–30 (2021).
4. Shao LY, Zhang JM, Chen XW et al. Artificial intelligence-driven distributed acoustic sensing technology and engineering application. *PhotoniX* **6**, 4 (2025).
5. Liu SQ, Yu FH, Hong R et al. Advances in phase-sensitive optical time-domain reflectometry. *Opto-Electron Adv* **5**, 200078 (2022).
6. Macedo L, Pedruzzi E, Avellar L et al. High-resolution sensors for mass deposition and low-frequency vibration based on phase-shifted Bragg gratings. *IEEE Sens J* **23**, 2228–2235 (2023).
7. Novotný V, Sysel P, Prokeš A et al. Fiber optic based distributed mechanical vibration sensing. *Sensors* **21**, 4779 (2021).
8. Zhang JM, Yan YX, Liu SQ et al. Adaptive block-matching and 3D denoising for Φ-OTDR under ultra-low SNR conditions. *J Lightwave Technol* **42**, 4698–4705 (2024).
9. Mu Q, Xu DY, Yu FH et al. Laser-frequency-drift compensation in Φ-OTDR using linear fitting intercepts method. *J Lightwave Technol* **43**, 8991–8997 (2025).
10. Han PY, Zhang JM, Chen XW et al. Explainable Riemannian manifold learning for application scene generalization with distributed acoustic sensing system. *IEEE Internet Things J* (2025). http://doi.org/10.1109/JIOT.2025.3586295.
11. Yu FH, Liu SQ, Xu DY et al. Data compression solution for ϕ-OTDR: encoding the extracted spectrum. *IEEE Sens J* **24**, 22429–22438 (2024).
12. Bencharif B, Erkorkmaz T. Distributed acoustic sensing for fence monitoring: deep learning approach for detection and classification of events on various types of fence. *Proc SPIE* **12272**, 1227205 (2022).
13. Wu HJ, Wang ZN, Peng F et al. Field test of a fully distributed fiber optic intrusion detection system for long-distance security monitoring of national borderline. *Proc SPIE* **9157**, 915790 (2014).
14. Tan DJ, Tian XZ, Sun W et al. An oil and gas pipeline pre-warning system based on Φ-OTDR. *Proc SPIE* **9157**, 91578W (2014).
15. Wijaya H, Rajeev P, Gad E et al. Automatic fault detection system for mining conveyor using distributed acoustic sensor.

Measurement **187**, 110330 (2022).
16. Becker M W, Harris B, Pevzner R. Characterization of aquifer poroelastic response to impulse and oscillatory well pressure using distributed acoustic sensing. *Geophys Res Lett* **50**, e2022GL100904 (2023).
17. Zhang SX, Li H, Fan CZ et al. Adaptive decentralized AI scheme for signal recognition of distributed sensor systems. *Opto-Electron Adv* **7**, 240119 (2024).
18. Jia HZ, Liang S, Lou SQ et al. A *k*-nearest neighbor algorithm-based near category support vector machine method for event identification of *φ*-OTDR. *IEEE Sens J* **19**, 3683–3689 (2019).
19. Fouda BMT, Yang B, Han DZ et al. Pattern recognition of optical fiber vibration signal of the submarine cable for its safety. *IEEE Sens J* **21**, 6510–6519 (2021).
20. Tejedor J, Macias-Guarasa J, Martins HF et al. A contextual GMM-HMM smart fiber optic surveillance system for pipeline integrity threat detection. *J Lightwave Technol* **37**, 4514–4522 (2019).
21. Wu HJ, Yang SQ, Liu XY et al. Simultaneous extraction of multi-scale structural features and the sequential information with an end-to-end mCNN-HMM combined model for fiber distributed acoustic sensor. *J Lightwave Technol* **39**, 6606–6616 (2021).
22. Lyu CG, Huo ZQ, Liu YG et al. Robust intrusion events recognition methodology for distributed optical fiber sensing perimeter security system. *IEEE Trans Instrum Meas* **70**, 9505109 (2021).
23. Xu WJ, Yu FH, Liu SQ et al. Real-time multi-class disturbance detection for Φ-OTDR based on YOLO algorithm. *Sensors* **22**, 1994 (2022).
24. Zhou ZX, Jiao WY, Hu X et al. Open-set event recognition model using 1-D RL-CNN with OpenMax algorithm for distributed optical fiber vibration sensing system. *IEEE Sens J* **23**, 12817–12827 (2023).
25. Wu HJ, Liu YM, Tu YL et al. Multi-source separation under two “blind” conditions for fiber-optic distributed acoustic sensor. *J Lightwave Technol* **40**, 2601–2611 (2022).
26. Wu HJ, Lu MY, Xu CY et al. Nonlinear mixture signal separation with the extended slow feature analysis (xSFA) in fiber-optic distributed acoustic sensor (DAS). *J Lightwave Technol* **42**, 2580–2594 (2024).
27. Gu HX, Liu SQ, Yu FH et al. Frequency domain separation of das multi-source aliased signals. In *2023 Asia Communications and Photonics Conference/2023 International Photonics and Optoelectronics Meetings* 1–4 (IEEE, 2023). http://doi.org/10.1109/ACP/POEM59049.2023.10369858.
28. Luo ZH, Yang Z, Chen XA et al. Separating method for multi-source vibration signals in ultra-weak fiber Bragg grating distributed acoustic sensors. *Opt Fiber Technol* **81**, 103501 (2023).
29. Shang LM, Cao JW, Wang JZ et al. Fundamental frequency energy distribution of periodic vibrations and their relation to distance. In *2016 IEEE 13th International Conference on Signal Processing* 96–101 (IEEE, 2016). http://doi.org/10.1109/ICSP.2016.7877804.
30. Luo Y, Chen Z, Yoshioka T. Dual-path RNN: efficient long sequence modeling for time-domain single-channel speech separation. In *2020 IEEE International Conference on Acoustics, Speech and Signal Processing* 46–50 (IEEE, 2020). http://doi.org/10.1109/ICASSP40776.2020.9054266.

Competing interests

The authors declare no competing financial interests.

Supplementary information

Supplementary information for this paper is available at https://doi.org/10.29026/oea.2025.240270

Scan for Article PDF